Pathway of bichromatic high-order harmonic generation

Jun Cai and Haoxue Qiao
Department of Physics, Wuhan University, Wuhan 430072, China
(Received 26 September 2006; published 6 March 2007)

We present a theoretical study of the pathway of harmonic generation in bichromatic linearly polarized laser fields. A "harmonic-collapse" phenomenon is observed in the power spectrum for a particular value of the amplitude ratio of two components of the external field. We employ an offset frequency shift to the additional field to distinguish the harmonic pathway and then to explain the harmonic-collapse phenomenon. The harmonic intensity as a function of the relative amplitude ratio and, furthermore, the fine structure of the harmonic spectrum can be well understood on the basis of a pathway analysis.

DOI: 10.1103/PhysRevA.75.035801 PACS number(s): 42.65.Ky, 32.80.−t

High-order harmonic generation (HHG) in intense laser fields has drawn great interest in recent decades for its ability to provide an efficient source of coherent extreme ultraviolet (XUV) and soft x-ray radiation. A lot of theoretical methods have been used to study the process of harmonic generation [1–5]. The main features of HHG such as an extended plateau comprising harmonics of comparable intensity and a sharp cutoff at the end of the plateau have been interpreted by using the semiclassical three-step model [6]. By adding an additional field to the fundamental one, the nonlinear spectra exhibit many new features—for example, with the combination of a fundamental field and its second order harmonic, both even and odd harmonics can be generated by sum and difference frequency mixing [7,8]. With respect to a comparison of the harmonic emission time and the classical return time, time-frequency analysis [9] of two-color high-order harmonic generation using quantum mechanical methods gives out strikingly coincident results with the semiclassical three-step model providing the two driving fields of commensurate intensity.

Discussions of the pathway of HHG in the bichromatic case have been mentioned in several papers. Some harmonics which cannot be observed in the monochromatic case can be generated in a bichromatic field by several possible pathways which should fulfill angular momentum conservation [10,11]. Gaarde *et al.* considered a two-color field consisting of a strong laser field and a much weaker field of variable frequency and calculated the harmonic spectrum generated by different sum and difference frequency mixing processes separately, in both the single-atom regime and propagation regime [12]. In a recent paper [13], an experimental study of nonlinear wave-mixing processes in extreme ultraviolet driving field by Misoguti *et al.* shows that the strong fundamental and the weak second-harmonic fields result in a nonlinear four-wave difference frequency-mixing process.

In this paper, we present a quantum mechanical calculation of HHG in a bichromatic field, whose two components are collinearly polarized along the z axis. We use the split-operator [4] pseudospectral method to solve the time-dependent Schrödinger equation (TDSE) of the hydrogen atom in spherical polar coordinates [5]. Once we obtain the time-dependent wave functions $\psi(\vec{r},t)$ in the external laser field, the time-dependent dipole moments in the acceleration form can be derived as

$$d_a(t) = \langle \psi(\vec{r},t) | -\frac{z}{r^3} + E(t) | \psi(\vec{r},t) \rangle \tag{1}$$

and the HHG power spectrum is calculated from the Fourier transform of the dipole moments:

$$P(\omega) = \left| \frac{1}{t_f - t_i} \frac{1}{\omega^2} \int_{t_i}^{t_f} d_a(t) e^{-i\omega t} dt \right|^2. \tag{2}$$

It has been pointed out that the harmonic spectrum calculated by the Fourier transform of the acceleration form of the dipole moments can avoid spurious background radiation [14]. It is extremely important to use the acceleration form of the dipole moments in our calculation for the position where the harmonic peaks appear should be determined precisely.

The bichromatic laser field can be described as a time-dependent electric field

$$E(t) = E_0 \sin^2\left(\frac{\pi}{\tau_p} t\right)[\sin(\omega_1 t) + \beta \sin(\omega_2 t)], \tag{3}$$

where τ_p is the pulse duration, the $\sin^2$ part of Eq. (3) describes the temporal envelop of the pulse, and β is the amplitude ratio of the additional field to the fundamental field. The parameters of the laser field are set as $E_0=0.045$ a.u. (7.08×10^{13} W/cm^2), the fundamental field frequency $\omega_1 = 3.0\omega_0$ ($\lambda_1=1064$ nm), where $\omega_0=0.0143$ a.u., the additional field frequency $\omega_2=5.0\omega_0$ ($\lambda_2=638$ nm), and the pulse duration $\tau_p=20\times\frac{2\pi}{\omega_0}$, which means 60 periods of the fundamental field. The amplitude ratio varies in different scenarios.

Figure 1 shows the power spectra of HHG under the bichromatic laser field with respect to different amplitude ratios. The insets are magnified views. In Fig. 1(a) the amplitude ratio is set to be $\beta=0.2$, while in Fig. 1(b), $\beta=0.35$, and in Fig. 1(c), $\beta=0.7$. The abscissa denotes the photon energy of the generated radiation in units of ω_0, while the y axis is the denary logarithm of the harmonic intensity. We treat the harmonic with the frequency $n\omega_0$ as the nth-order harmonic. Only odd-order harmonics with the frequency $(2n+1)\omega_0$ can be observed for the reflection symmetry is preserved [8]. Here, we focus on the 15th-order harmonic generation. In Figs. 1(a) and 1(c), this order harmonic peak can be clearly observed. But when $\beta=0.35$, the 15th-

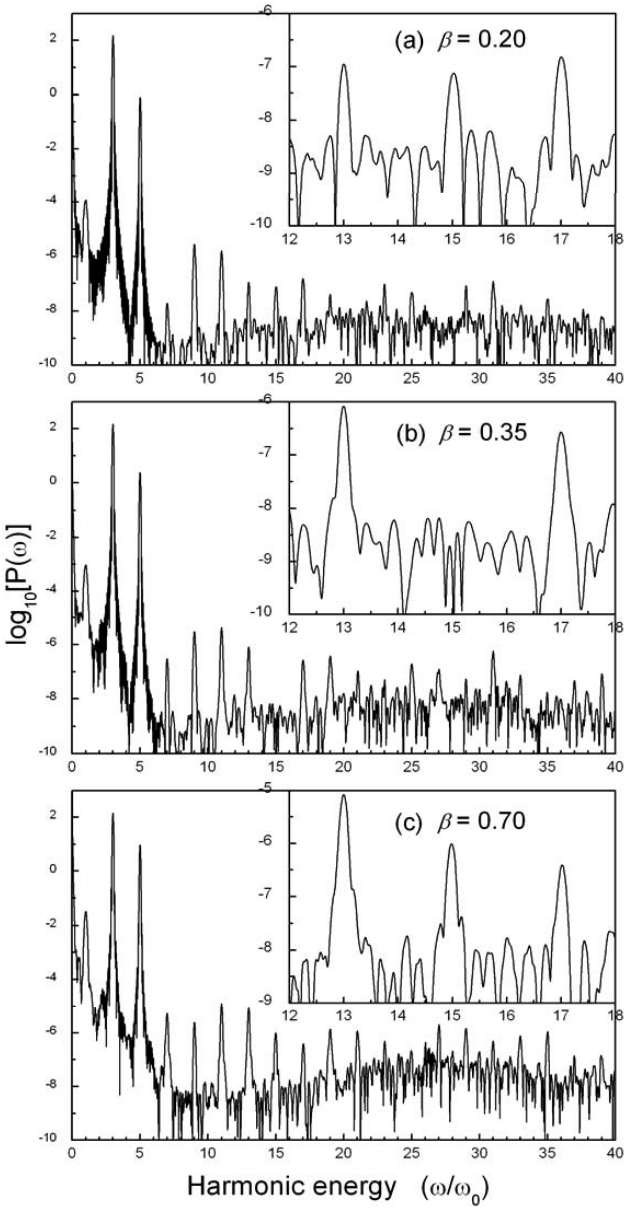

FIG. 1. The acceleration form power spectra scale from 0 to $40\omega_0$ for the amplitude ratio (a) β=0.2, (b) β=0.35, and (c) β =0.7. Other parameters are chosen as E_0=0.045 a.u., $\omega_1=3.0\omega_0$, $\omega_2=5.0\omega_0$, and $\tau_p=20\times\frac{2\pi}{\omega_0}$. The insets are magnified views scaling from $12\omega_0$ to $18\omega_0$.

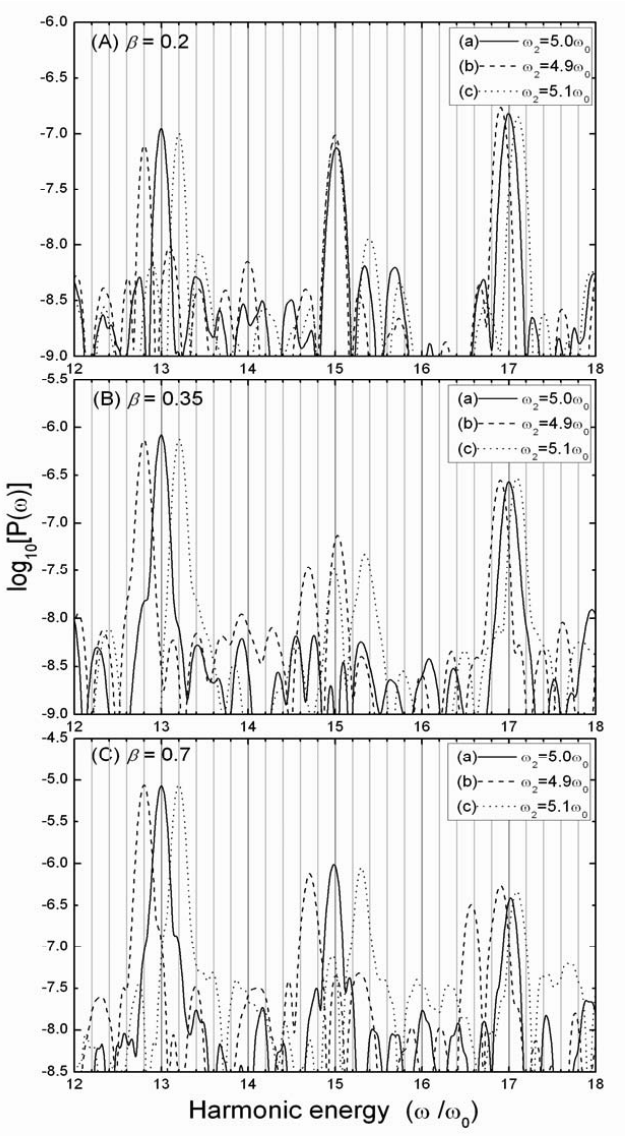

FIG. 2. The acceleration form power spectra for the amplitude ratio (A) β=0.2, (B) β=0.35, and (C) β=0.7 and the frequency of the additional laser field (a) $\omega_2=5.0\omega_0$ (solid line), (b) $\omega_2=4.9\omega_0$ (dashed line), and (c) $\omega_2=5.1\omega_0$ (dotted line) for comparison, while other parameters are chosen the same as in Fig. 1.

harmonic intensity is extremely weak and the harmonic peak is submerged in the background radiation in Fig. 1(b). We regard this phenomenon as "harmonic collapse" in the power spectrum of the bichromatic field. However, the shape of whole high-order harmonic is similar to other calculations; the harmonic collapse is only present at a certain position for a particular amplitude ratio of the two components of the laser field.

In order to interpret this phenomenon, we investigate the pathway of harmonic generation, and the quantum interference between different pathways maybe the reason for the harmonic collapse. A frequency variation is added to the additional field:

$$\omega_2 = 5.0\omega_0 + \Delta\omega, \tag{4}$$

where $\Delta\omega$ is much smaller than ω_0. Figure 2 shows the power spectra of HHG when the frequency of the additional laser field is set to be (a) $\omega_2=5.0\omega_0$ (same as in Fig. 1), (b) $\omega_2=4.9\omega_0$, and (c) $\omega_2=5.1\omega_0$ ($\Delta\omega=\pm0.1\omega_0$), respectively. Other parameters are set the same as in Fig. 1. According to the frequency variation of the additional field, the harmonic peaks have frequency shifts, they appear near $(2n+1)\omega_0$, and some peaks still have almost the same intensity with the peaks generated in case (a). We have calculated harmonic generation for $\Delta\omega$ varying from $0.01\omega_0$ to $0.1\omega_0$; similar phenomena are observed. Here we choose $\Delta\omega$ to be $0.1\omega_0$ for the sake of simplicity in discussion.

In Fig. 2(A), the harmonic of frequency $13\omega_0$ (13th-order

harmonic) is generated in case (a), while the main harmonic peaks appear at $12.8\omega_0$ and $13.2\omega_0$ with respect to different additional field frequencies $\omega_2=4.9\omega_0$ and $\omega_2=5.1\omega_0$. The offset frequency shifts in cases (b) and (c) are $0.2\omega_0$, which means 2 times $\Delta\omega$. So the additional field contributes two photons to the 13th-harmonic generation. The harmonic of $13\omega_0$ is generated by absorbing one photon from the fundamental field ($1\times 3\omega_0$) and two photons from the additional field ($2\times 5\omega_0$). The leading pathway of target atom H absorbing photons from the bichromatic field to generate 13th-order harmonic can be denoted by

$$H+\gamma(3\hbar\omega_0)+2\gamma(5\hbar\omega_0)\rightarrow H+\gamma(13\hbar\omega_0). \quad (5)$$

There are secondary pathways to generate the 13th harmonic—for example,

$$H+6\gamma(3\hbar\omega_0)-\gamma(5\hbar\omega_0)\rightarrow H+\gamma(13\hbar\omega_0). \quad (6)$$

Through this difference frequency mixing process [12], the harmonic peak should appear at $13.1\omega_0$ in case (b) $\omega_2=4.9\omega_0$ and $12.9\omega_0$ in case (c) $\omega_2=5.1\omega_0$. These subpeaks can also be observed in the harmonic spectra, but they are weaker by an order of magnitude in intensity comparing with the main peaks. The harmonic peaks still appear at $15\omega_0$ in cases (b) and (c) though the additional field frequency changed to be $4.9\omega_0$ and $5.1\omega_0$. So the 15th-order harmonic is generated by absorbing five photons from the fundamental field:

$$H+5\gamma(3\hbar\omega_0)\rightarrow H+\gamma(15\hbar\omega_0). \quad (7)$$

A similar analysis can be applied to the 17th harmonic; its leading pathway can be written as

$$H+4\gamma(3\hbar\omega_0)+\gamma(5\hbar\omega_0)\rightarrow H+\gamma(17\hbar\omega_0). \quad (8)$$

The leading pathway of the 13th- and 17th-order harmonic remains unchanged in Figs. 2(B) and 2(C). But to the 15th harmonic, in Fig. 2(C), the main harmonic peaks appear at $14.7\omega_0$ in case (b) and $15.3\omega_0$ in case (c), which means the leading pathway of the 15th harmonic changed to be

$$H+3\gamma(5\hbar\omega_0)\rightarrow H+\gamma(15\hbar\omega_0). \quad (9)$$

In Fig. 2(B), the 15th-order harmonic peak cannot be observed in case (a) but there are harmonic peaks appearing at $14.7\omega_0$ and $15\omega_0$ in case (b) and $15.3\omega_0$ and $15\omega_0$ in case (c). So we can conclude that the two different pathways denoted by formulas (7) and (9) have commensurate contributions to the 15th-order harmonic generation, and the interference of two pathways decreases the 15th-harmonic intensity. While in cases (b) and (c), the frequency variation of the additional field destroys the coherence condition of the two pathways, so the harmonic collapse phenomenon disappears and the harmonic peaks generated by different pathways are preserved in the power spectrum.

The harmonic collapse phenomenon can be observed in other order harmonics. For example, in the low-amplitude ratio region, the 29th harmonic's leading pathway is

$$H+8\gamma(3\hbar\omega_0)+\gamma(5\hbar\omega_0)\rightarrow H+\gamma(29\hbar\omega_0), \quad (10)$$

and the leading pathway changes to be

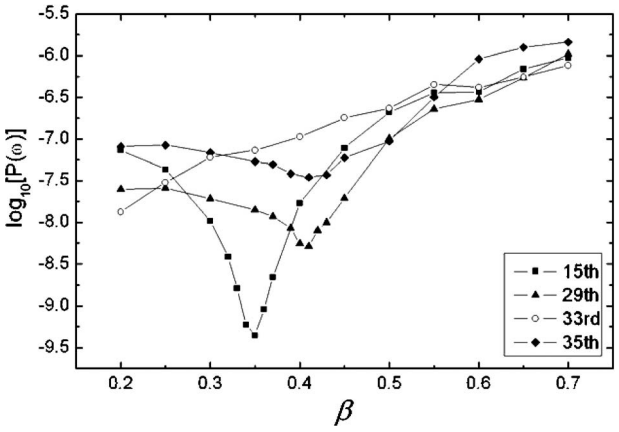

FIG. 3. Intensities of the 15th-, 29th-, 33rd-, and 35th-order harmonics as functions of the amplitude ratio for the additional field frequency $\omega_2=5.0\omega_0$.

$$H+3\gamma(3\hbar\omega_0)+4\gamma(5\hbar\omega_0)\rightarrow H+\gamma(29\hbar\omega_0) \quad (11)$$

when the additional field becomes stronger. The coherence of the two different pathways causes the decrease of the 29th harmonic. A similar phenomenon can be observed in the 35th harmonic, whose two different leading pathways can be denoted by

$$H+10\gamma(3\hbar\omega_0)+\gamma(5\hbar\omega_0)\rightarrow H+\gamma(35\hbar\omega_0) \quad (12)$$

and

$$H+5\gamma(3\hbar\omega_0)+4\gamma(5\hbar\omega_0)\rightarrow H+\gamma(35\hbar\omega_0). \quad (13)$$

Figure 3 gives an overview of the 15th-, 29th-, 33rd-, and 35th-order harmonic intensities when the amplitude ratio of the additional field to the fundamental field set to different values. The additional field frequency is set to be $\omega_2=5.0\omega_0$. The leading pathway of the 33rd harmonic is

$$H+6\gamma(3\hbar\omega_0)+3\gamma(5\hbar\omega_0)\rightarrow H+\gamma(33\hbar\omega_0), \quad (14)$$

and it remains unchanged in the region $\beta=0.2\sim 0.7$. In Fig. 3, the intensity line of the 33rd harmonic (open circles) rises with the larger amplitude ratio. However, the intensity lines of the 15th, 29th, and 35th harmonics (solid curves) show a "valley" shape. To these order harmonics, they have different leading pathways at the two ends of the intensity line. In the middle region, the coherent effect of two different pathways decreases the harmonic intensity. For example, as has been depicted in Fig. 2(A), the 15th-order harmonic has the intensity of the same order of magnitude comparing with its neighboring harmonics for its leading pathway can be distinguished from other pathways in the region $\beta=0.1-0.2$; the intensity line shows a decline in the region $\beta=0.2-0.35$ though the additional field becomes stronger; the harmonic intensity reaches its minimum when $\beta=0.35$ and the harmonic collapse phenomenon appears; in the region $\beta=0.35-0.7$, the pathway denoted by formula (9) gradually becomes dominant in the 15th-order harmonic generation and the harmonic intensity increases as the increasing intensity of the additional field.

When other parameters of the external field changed, for example, for different amplitude of the field E_0 or different pulse duration τ_p of the laser pulse, or when the two field components have a relative phase difference and different shape of laser pulse, the harmonic collapse phenomenon can still be observed, but the amplitude ratio where the harmonic peak is missing changes. A detailed study of HHG and its pathways in these different scenarios still needs to be done.

In summary, we investigated the pathway of harmonic generation in two collinearly polarized laser fields with frequency ratio 3:5. The frequency shift of harmonic peaks caused by the additional field frequency variation illustrates the pathway of harmonic generation. To most orders of harmonic generation, there exists a leading pathway which contributes most to the harmonic intensity, and the harmonic peak can be clearly observed. But when two different pathways have commensurate contributions to the harmonic generation simultaneously, the harmonic intensity is much weaker compared with its neighboring harmonics. Especially when the relative intensity of the two components of the bichromatic field is suitable, the harmonic peak can be submerged in background radiation and the "harmonic collapse" phenomenon is observed. However, the shape of whole high-order harmonic is similar to other calculations; the harmonic collapse is only present at a certain position for a particular amplitude ratio of the two components of the laser field. By using an offset frequency shift of the additional field to destroy the coherent condition of the two pathways, we can see that the harmonic peaks generated through different pathways appear (as seen in Fig. 2). Therefore, this harmonic collapse may be caused by the quantum interference of different pathways. An advanced study is in progress.

We would like to thank Liangwen Pi and Xiaofeng Wang for helpful discussions. This work was supported by the National Natural Science Foundation of China under Grant No. 10374074.

[1] M. Lewenstein, Ph. Balcou, M. Yu. Ivanov, Anne L'Huillier, and P. B. Corkum, Phys. Rev. A **49**, 2117 (1994).
[2] Haoxue Qiao, Qingyu Cai, Jianguo Rao, and Baiwen Li, Phys. Rev. A **65**, 063403 (2002).
[3] Dejan B. Milošević, Wilhelm Becker, and Richard Kopold, Phys. Rev. A **61**, 063403 (2000).
[4] Mark R. Hermann and J. A. Fleck, Jr., Phys. Rev. A **38**, 6000 (1988).
[5] X.-M. Tong and S.-I. Chu, Chem. Phys. **217**, 119 (1997).
[6] P. B. Corkum, Phys. Rev. Lett. **71**, 1994 (1993).
[7] E. E. Aubanel and A. D. Bandrauk, Chem. Phys. Lett. **229**, 169 (1994).
[8] T. Zuo, A. D. Bandrauk, M. Ivanov, and P. B. Corkum, Phys. Rev. A **51**, 3991 (1995).
[9] C. Figueira de Morisson Faria, M. Dörr, W. Becker, and W. Sandner, Phys. Rev. A **60**, 1377 (1999).
[10] H. Eichmann, A. Egbert, S. Nolte, C. Momma, B. Wellegehausen, W. Becker, S. Long, and J. K. McIver, Phys. Rev. A **51**, R3414 (1995).
[11] H. Eichmann, S. Meyer, K. Riepl, C. Momma, and B. Wellegehausen, Phys. Rev. A **50**, R2834 (1994).
[12] M. B. Gaarde, A. L'Huillier, and M. Lewenstein, Phys. Rev. A **54**, 4236 (1996).
[13] L. Misoguti, I. P. Christov, S. Backus, M. M. Murnane, and H. C. Kapteyn, Phys. Rev. A **72**, 063803 (2005).
[14] K. Burnett, V. C. Reed, J. Cooper, and P. L. Knight, Phys. Rev. A **45**, 3347 (1992).